# TIME OF REMEDIATION ESTIMATES

## Enhanced Bioremediation at ST012

Date: May 16, 2017

Prepared By: Lloyd "Bo" Stewart, PhD, PE
Praxis Environmental Technologies, Inc., Burlingame, CA

---

***OUTLINE***

**Executive Summary**

1. **Conceptual Site Model Summary**

2. **NAPL Volume Estimates for EBR and NAPL Composition**

3. **Endpoint for Modeling Remediation**

4. **Idealized Model of NAPL Depletion Assuming Groundwater-NAPL Equilibrium**

5. **Screening-Level NAPL Depletion Models**
   - ***5.1. NAPL Depletion Calculations for First Order Degradation***
   - ***5.2. NAPL Depletion Calculations for Sulfate Reduction with Monod Kinetics***

6. **Phase I Feasibility and Implementation Issues**

**References**

**Appendix A. Depletion of Two-Component NAPL Assuming Equilibrium**

**Appendix B. Volume-Averaged Depletion of Multi-Component NAPL Source Zones**

***PREAMBLE***

This memorandum is intended to frame discussion on expectations from the field implementation of sulfate reduction. The purpose of the modeling is to provide order-of-magnitude estimates for the duration of treatment required to attain remedial goals. The memorandum presents theoretical modeling results - mathematical relationships describing processes in the subsurface with estimated parameter inputs. Disagreement on the modeling results should center on what the model does and does not include, what the model assumes, and appropriate input parameters based on field observations. Accuracy is not implied by the number of significant digits presented in the memo, these are only for relative comparisons.



ED_005025_00013390-00001

## *EXECUTIVE SUMMARY*

This memorandum describes a screening level evaluation of enhanced bioremediation (EBR) applied to NAPL source zone targets outside the SEE treatment zones at ST012. The model is based on a mass balance for the NAPL source zones. Contaminants dissolve out of the NAPL into surrounding groundwater and then undergo biological degradation. Remediation is complete when contaminant fractions in the NAPL are reduced to levels that no longer impact groundwater above cleanup goals. The duration to attain this goal is known as the time of remediation (TOR). The evaluation assumes a range of initial conditions and applies three bioremediation models of varying complexity. Sulfate reduction was selected as the bioremediation process to be enhanced with the underlying assumption that the addition of sulfate will accelerate the degradation of contaminants.

Detailed numerical calculations for monitored natural attenuation before and following a hypothetical application of SEE were performed previously using the SEAM3D Model and are presented in Appendix M of the TEE Pilot Test Evaluation Report (BEM, 2011). Those calculations were very complex; however, depletion of individual source zones can be estimated to the same order-of-magnitude with straightforward mass balances that include the same mechanisms of remediation averaged over each target NAPL source soil volume. Details of the volume-averaged model are provided in Appendix B.

Calculated times of remediation (TOR) for untreated EBR targets are summarized in Table ES1 based on depleting benzene from NAPL with sulfate reduction to levels equivalent to MCL using a model of Monod kinetics, NAPL volume estimates from Amec Worksheets, and an initial sulfate concentration of 8,000 mg/L. The four scenarios presented are based on four different approaches to estimating the residual NAPL volume remaining (calculated saturation, literature saturation and two different total soil porosities). The timeframes assume EBR is operated until RAOs are attained without follow-on MNA (shortest timeframe). Results for first order degradation with a sustained decay constant of 0.0125 day$^{-1}$ are included for comparison.

**Table ES1. TOR for NAPL Depletion with Sulfate Reduction**

| **Aquifer Zone – Kinetics** | **Ambient Flow** gpm | **Calculated Target NAPL Volume** Porosity=0.3 **years** | **Calculated Target NAPL Volume** Porosity=0.4 **years** | **Literature Target NAPL Volume** Porosity=0.3 **years** | **Literature Target NAPL Volume** Porosity=0.4 **years** | **Note** |
|---|---|---|---|---|---|---|
| UWBZ – 1st Order | 4.4 | 17.0 | 11.4 | 19.8 | 20.3 | Note 1 |
| UWBZ – Monod | 4.4 | 100 | 92 | 111 | 136 | Note 2 |
| LSZ – 1st Order | 3.5 | 13.7 | 9.4 | 26.9 | 29.2 | Note 1 |
| LSZ – Monod | 3.5 | 9.5 | 8.0 | 17.7 | 22.6 | Note 3 |

* Zero ambient flow is included to mimic recirculation wherein sulfate is not lost with groundwater exiting the target soil volume.

Note 1: Calculated with a first order degradation rate constant of 0.0125 d$^{-1}$, assumed to be applicable for all time independent of sulfate concentration and biomass conditions.



ED_005025_00013390-00002

Note 2: For a background death rate of 0.001 $d^{-1}$, the microbial population did not grow, the injected sulfate was not utilized, and the TOR was over 200 years based primarily on the dissolved phase exiting the source soil volume. Setting the background microbial death rate to 0 yielded a TOR of 92-136 years by allowing the biomass to grow slowly (limited by the utilization rate); very little of the injected sulfate was utilized.

Note 3: The initial distribution of excess sulfate (8,000 mg/L) was utilized or washed out of the soil volume in 3 to 3.6 years; however, the microbial concentration grew and utilized ambient sulfate entering the volume to complete the process along with dissolved mass flowing out of the volume. Assuming a microbial background death rate of zero shortened the TOR by 1 to 2 years.

Based on the model and underlying assumptions, the concentration of sulfate reducing bacteria grew to a stationary phase concentration around 3 to 3.5 mg/L in both zones, when growth occurred. The growth period was approximately 12 to 24 months in the LSZ. The growth period in the UWBZ was on the order of 35 to 40 years assuming a zero death rate. The UWBZ growth was slow and the results were very sensitive to the death rate as a result of the low utilization rate. The calculated TOR was not strongly influenced by the assumed initial biomass concentration (0.01 mg/L). Based on the model NAPL compositions, initial sulfate concentrations exceeding 8,000 mg/L provided no improvement in the TOR and concentrations above 4,000 mg/L may begin to inhibit sulfate reduction (Al-Zuhair et al., 2008).

Conditions in the UWBZ are known to be evolving (BEM, 2011); therefore, calculations for the UWBZ were repeated assuming subsurface conditions could be manipulated to improve utilization rates of hydrocarbons by a factor of ten over the calibrated values from 2011. The results are provided below in Table ES2. Timeframes are shortened to be within the same order as calculated for the LSZ but remain longer.

**Table ES2. TOR for UWBZ NAPL Depletion with Sulfate Reduction (Utilization x 10)**

| **Aquifer Zone – Kinetics** | **Ambient Flow** gpm | **Calculated Target NAPL Volume** Porosity=0.3 **years** | **Calculated Target NAPL Volume** Porosity=0.4 **years** | **Literature Target NAPL Volume** Porosity=0.3 **years** | **Literature Target NAPL Volume** Porosity=0.4 **years** |
|---|---|---|---|---|---|
| UWBZ – Monod ($\upsilon_i^{max}$ Table 8) | 4.4 | 100 | 92 | 111 | 136 |
| UWBZ – Monod ($\upsilon_i^{max}$x10) | 4.4 | 28.7 | 17.0 | 35.1 | 43.1 |

## 1. Conceptual Site Model Summary

A comprehensive conceptual site model (CSM) including the UWBZ, LPZ and LSZ is presented in Appendix A of the TEE Pilot Test Evaluation Report (BEM, 2011). The geologic materials in the saturated zone are subdivided into five main hydrostratigraphic units described from the bottom upwards (BEM, 2003):

- The Aquitard, occurring at approximately 260 ft to 245 ft bgs;
- The LSZ extending from approximately 245 ft to 210 ft bgs;
- The LPZ, extending from approximately 210 ft to 195 ft bgs;
- The UWBZ, extending from approximately 195 to 160 ft bgs; and
- The Cobble Zone, extending from approximately 160 ft to 145 ft.

Lithologic descriptions of the zones can be found in Table A.3.3.1.1 1 (BEM, 2011). In January 2010 the water table at Site ST012 was approximately 158 ft bgs and rising at an average rate of 3.4 ft per year. The horizontal gradient of both the LSZ and UWBZ averaged 0.005 feet per foot (ft/ft) toward the east.

In 1998, two pumping tests were conducted in the LSZ after it became completely saturated (BEM, 1998a). The conductivity values derived from these pumping tests ranged from 18 ft/day to 40 ft/day. In 2006, an aquifer test was conducted and analyzed using five different methods for hydraulic conductivity. Results provided an average conductivity of 37.7 ft/day. Similar conductivity values (about 40 ft/day) were derived from a pumping test performed in June 2003 (BEM, 2006). Mean hydraulic conductivity for the calibrated LSZ groundwater flow model of 2011 (BEM, 2011, Appendix M) was 16 ft/day. In the UWBZ, previous modeling with SEAM3D (BEM, 2011, Appendix M) assumed a mean hydraulic conductivity of 12.7 ft/day and slug test modeling by HGL yielded an estimate of 13.4 ft/day (HGL, 2005).

Similar site gradients are reported in Appendix E of the Draft Final ST012 RDRA Work Plan Addendum #2 for EBR (Amec Foster Wheeler, March 2016). However, the hydraulic conductivity values of 3 and 1.5 ft/day for the LSZ and UWBZ, respectively, in Appendix E are significantly lower than in previous modeling. Appendix E presents an hydraulic conductivity of 70 ft/day for the CZ. The site hydrogeologic properties for the present modeling are summarized in Table 1. The hydraulic conductivities employed in the BEM modeling of 2011 for the UWBZ and LSZ are employed. The NAPL-impacted soil volume and transect widths in Table 1 are those reported in Appendix E and represent pre-SEE conditions.

**Table 1. Pre-SEE Source Zone Physical Properties and Dimensions**

| Aquifer Zone | NAPL-Impact Soil Volume^ $V_S$ yd^3 | Transect Width W ft | Thickness* Z ft | Hydraulic Conductivity ft/day | Ambient GW Velocity U ft/day | Ambient GW Flow Q gpm |
|---|---|---|---|---|---|---|
| CZ | 40,000 | 220 | 15 | 70 | 0.343 | 5.9 |
| UWBZ | 153,000 | 320 | 35 | 12.7 | 0.0635 | 3.7 |
| LPZ | 122,600 | - | 15 | - | - | - |
| LSZ | 241,200 | 355 | 24* | 16 | 0.080 | 3.6 |

^ The NAPL-impacted soil volumes were taken from Appendix A (BEM, 2011)
* The LSZ thickness impacted by NAPL is assumed to be 234 – 210 ft bgs = 24 ft
Note: The horizontal gradient for all zones is assumed to be 0.005 ft/ft
Note: Baseline porosity for all zones is assumed to be 0.30

The total ambient flow of groundwater through each zone (Q) depends upon the thickness (Z) and width (W) of the NAPL-impacted soil in each zone perpendicular to the direction of groundwater flow as well as the soil porosity ($\phi$=0.30). The total flow through each zone, Q, is listed in Table 1 and calculated as follows:

$$Q = v_s \varphi Z W = U Z W$$

For the EBR evaluation, the initial target NAPL-impacted soil volumes are assumed to be the areas untreated by SEE and those assumed to be in the SEE radius of influence but outside any thermal influence. The target volumes were determined from the total NAPL-impacted soil volume for each zone presented in Mass Extent Evaluation Worksheet "Post-SEE mass" and the soil volumes presented for the TTZ and TIZ. The calculated target EBR soil volumes are listed in Table 2 and illustrated in Figures 1 through 3 for the CZ, UWBZ and LSZ. Estimated transect widths are also illustrated in the figures and included in Table 2 to estimate the ambient groundwater flows through the target volumes.

**Table 2. Physical Properties and Dimensions of Initial EBR-Targeted Source Zones**

| Aquifer Zone | Target NAPL Soil Volume^ $V_s$ yd^3 | Transect Width W ft | Thickness Z ft | Hydraulic Conductivity ft/day | Ambient GW Velocity U ft/day | Ambient GW Flow Q gpm |
|---|---|---|---|---|---|---|
| CZ | 3,139 | 120 | 15 | 70 | 0.343 | 3.2 |
| UWBZ | 122,556 | 380 | 35 | 12.7 | 0.0635 | 4.4 |
| LPZ | 42,616 | - | 15 | - | - | - |
| LSZ | 38,500 | 350 | 24* | 16 | 0.080 | 3.5 |

^ Target NAPL soil volumes calculated from Mass Extent Evaluation Worksheet "Post-SEE mass" by subtracting TTZ and TIZ from Total for each zone.

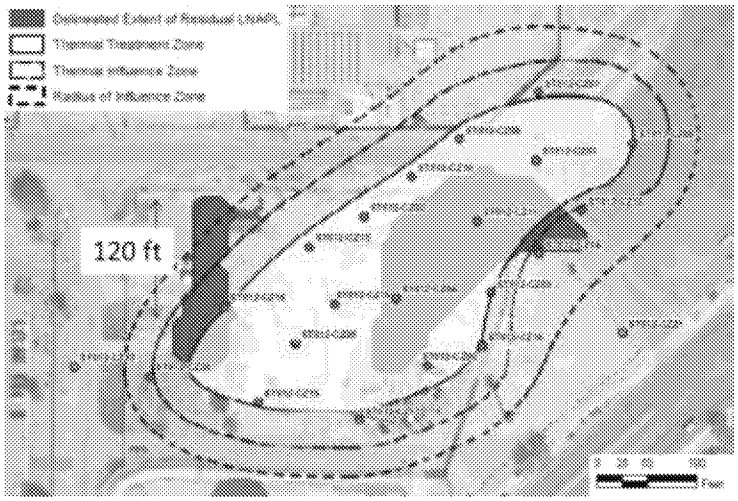


**Figure 1. Conceptual Model for EBR CZ NAPL Depletion (Mass Extent Evaluation Figure 2)**

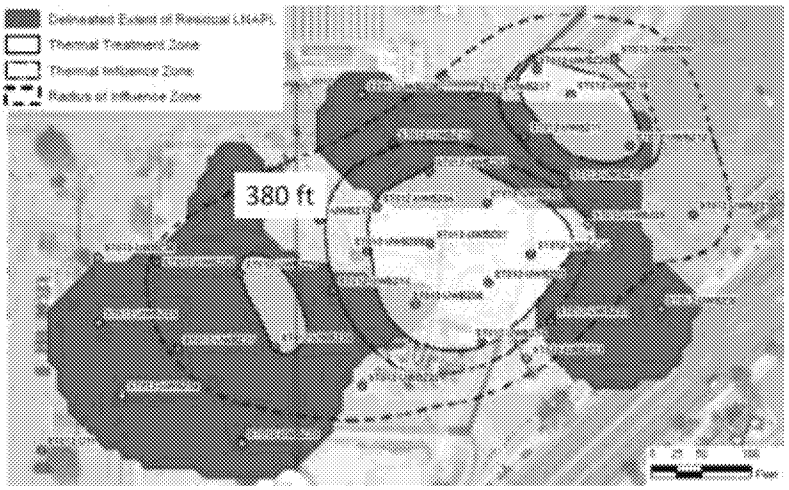


**Figure 2. Conceptual Model for EBR UWBZ NAPL Depletion (Mass Extent Evaluation Figure 4)**

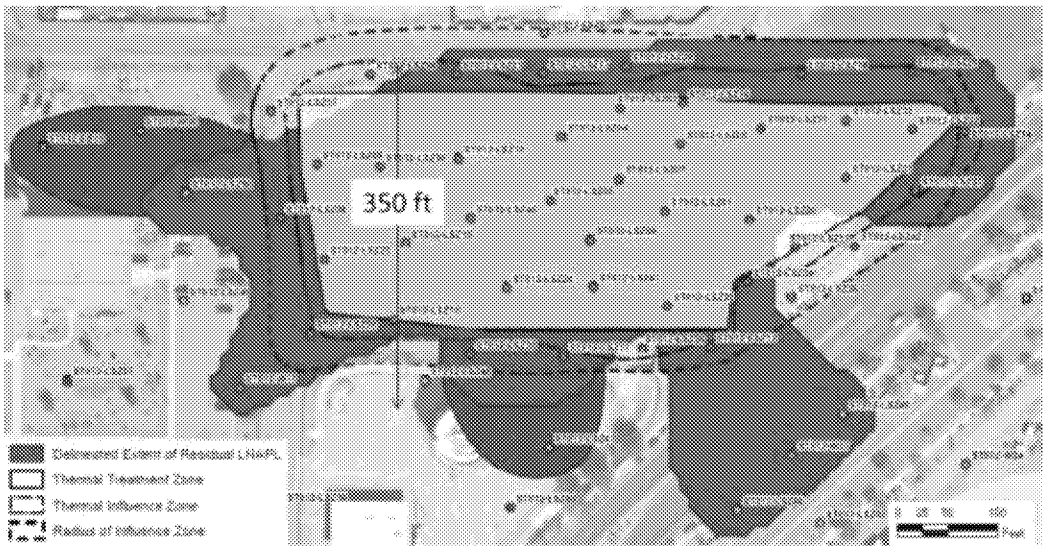


**Figure 3. Conceptual Model for EBR LSZ NAPL Depletion (Mass Extent Evaluation Figure 8)**

## 3. NAPL Volume Estimates for EBR and NAPL Composition

Target NAPL volume estimates for EBR in each zone were calculated similarly to the soil volumes described above. For this TOR evaluation, the initial target NAPL volumes are assumed to be those from areas untreated by SEE and those assumed to be in the SEE radius of influence but outside any thermal influence. The target NAPL volumes were determined from the NAPL volumes for each zone presented in Mass Extent Evaluation Worksheet "Post-SEE Mass." The calculated target NAPL volumes are listed in Table 3 and correspond to the areas illustrated in Figures 1 through 3 for the CZ, UWBZ and LSZ. Four scenarios presented are based on four different approaches to estimating the residual NAPL volume remaining (calculated saturation, literature saturation and two different total soil porosities). The Mass Extent Evaluation Worksheet assumed a total soil porosity of 0.3 and Table 3 includes NAPL estimates based on the same saturations but calculated with a total soil porosity of 0.4.

**Table 3. Initial EBR-Targeted NAPL Volume**

| Aquifer Zone | Target NAPL Soil Volume $V_S$ yd^3 | Calculated^ Target NAPL Volume Porosity=0.3 gal | Calculated^ Target NAPL Volume Porosity=0.4 gal | Literature* Target NAPL Volume Porosity=0.3 gal | Literature* Target NAPL Volume Porosity=0.4 gal |
|---|---|---|---|---|---|
| CZ | 3,139 | 2,663 | 2,282 | 1,902 | 2,536 |
| UWBZ | 122,556 | 250,999 | 215,142 | 294,399 | 395,887 |
| LSZ | 38,500 | 54,821 | 46,989 | 110,682 | 155,783 |

^ Target NAPL volumes estimated from calculations for residual saturation based on measured soil TPH concentrations.

* Target NAPL volumes estimated from literature values for residual saturation.

Based on various chemical analyses, different NAPL compositions were developed for the UWBZ and the LSZ for modeling in the TEE Pilot Test Evaluation. The pre-SEE model compositions for the UWBZ and LSZ are listed in Tables 4 and 5, respectively, and the mass fractions are taken directly from Table 4.1.1.1 (BEM, 2011). The UWBZ was unsaturated at the time of NAPL release and was subjected to soil vapor extraction from 1997 to 2003. The rising water table entered the bottom of the UWBZ (~195 ft bgs) during 1998 and reached the fine-grained unit separating the top of the UWBZ from the overlying CZ (~172 ft bgs) in 2004. Hence, the residual NAPL in the UWBZ was initially weathered by natural volatilization and further weathered by soil vapor extraction before becoming submerged. The result is a lower mass fraction of volatile compounds than found in the deeper LSZ NAPL that was weathered primarily by dissolution, a slower process.



ED_005025_00013390-00007

**Table 4. Model NAPL Composition for the UWBZ and Solubility at 25 C**

| C# | NAPL Component / Surrogate Compound | Mass Fraction, % | Mole Fraction, y | Pure Solubility, $C^{sat}$ (mg/L) | | Equilibrium Concentration, $C^{eq}$ (mg/L) |
|---|---|---|---|---|---|---|
| Aromatic Compounds of Concern | | | | | | |
| 6 | Benzene | 0.222 | 0.00347 | 1790 | | 6.21 |
| 7 | Toluene | 0.73 | 0.00966 | 526 | | 5.08 |
| 8 | Ethylbenzene | 0.97 | 0.01114 | 169 | | 1.88 |
| 8 | m&p-Xylenes | 1.73 | 0.01987 | 161 | | 3.20 |
| 8 | o-Xylene | 0.62 | 0.00712 | 178 | | 1.27 |
| 10 | Naphthalene* | 0.57 | 0.00542 | 31 | | 0.56 |
| Other Aromatic Constituents | | | | | | |
| 9 | 1,2,4-Trimethylbenzene | 2.00 | 0.02029 | 57 | | 1.16 |
| 9 | 1,3,5-Trimethylbenzene | 0.45 | 0.00456 | 48 | | 0.220 |
| 9 | 1-Methyl-3-ethylbenzene | 1.86 | 0.01890 | 35 | | 0.667 |
| 9 | Isopropylbenzene | 0.28 | 0.00284 | 61 | | 0.174 |
| 9 | n-Propylbenzene | 0.38 | 0.00385 | 52 | | 0.201 |
| 10 | 1,2,3,5-Tetramethylbenzene | 6.77 | 0.06151 | 28 | | 1.72 |
| 11 | 1-Methylnaphthalene | 2.72 | 0.02334 | 25 | | 0.584 |
| Isoalkanes | | | | | | |
| 6 | 2-Methylpentane | 0.09 | 0.00129 | 14 | | 0.018 |
| 7 | 2-Methylhexane | 2.94 | 0.03576 | 4.4 | | 0.158 |
| 8 | 3-Methylheptane | 13.79 | 0.14716 | 1.5 | | 0.215 |
| 9 | 2-Methyloctane | 10.34 | 0.09832 | 0.48 | | 0.047 |
| Cycloparaffins | | | | | | |
| 6 | Cyclohexane | 2.70 | 0.03915 | 55 | | 2.15 |
| 7 | Methylcyclohexane | 7.02 | 0.08716 | 17 | | 1.48 |
| 8 | Dimethylcyclohexane | 3.44 | 0.03735 | 8.4 | | 0.314 |
| 9 | Isopropylcyclohexane | 6.53 | 0.06307 | 3.1 | | 0.196 |
| n-Alkanes | | | | | | |
| 5 | n-Pentane | 0.00 | 0.00000 | 38 | | 0.000 |
| 6 | n-Hexane | 0.28 | 0.00397 | 9.5 | | 0.038 |
| 7 | n-Heptane | 3.48 | 0.04232 | 3.4 | | 0.164 |
| 8 | n-Octane | 5.48 | 0.05846 | 0.41 | | 0.039 |
| 9 | n-Nonane | 4.81 | 0.04568 | 0.22 | | 0.010 |
| 10 | n-Decane | 4.83 | 0.04143 | 0.052 | | 0.022 |
| 11 | n-Undecane | 5.26 | 0.04104 | 0.0044 | | 1.81E-04 |
| 12 | n-Dodecane | 4.57 | 0.03268 | 0.0037 | | 1.21E-04 |
| 13 | n-Tridecane | 3.48 | 0.02299 | 0.0029 | | 6.67E-05 |
| 14 | n-Tetradecane | 1.66 | 0.01021 | 0.0022 | | 2.25E-05 |
| TOTAL | | 100 | 1.0000 | | | 27.7 |

*Naphthalene has a fugacity ratio of 3.3 (solid at 25 C)

**Table 5. Model NAPL Composition for the LSZ and Solubility at 25 C**

| C# | NAPL Component / Surrogate Compound | Mass Fraction, % | Mole Fraction, y | Pure Solubility, $C^{sat}$ (mg/L) | | Equilibrium Concentration, $C^{eq}$ (mg/L) |
|---|---|---|---|---|---|---|
| Aromatic Compounds of Concern | | | | | | |
| 6 | Benzene | 0.83 | 0.0116 | 1790 | | 20.7 |
| 7 | Toluene | 2.90 | 0.0342 | 526 | | 18.0 |
| 8 | Ethylbenzene | 1.40 | 0.0143 | 169 | | 2.42 |
| 8 | m&p-Xylenes | 2.20 | 0.0225 | 161 | | 3.63 |
| 8 | o-Xylene | 0.83 | 0.0085 | 178 | | 1.51 |
| 10 | Naphthalene* | 0.50 | 0.0042 | 31 | | 0.13 |
| Other Aromatic Constituents | | | | | | |
| 9 | 1,2,4-Trimethylbenzene | 1.10 | 0.0100 | 57 | | 0.57 |
| 9 | 1,3,5-Trimethylbenzene | 0.37 | 0.0033 | 48 | | 0.16 |
| 9 | 1-Methyl-3-ethylbenzene | 1.15 | 0.0104 | 35 | | 0.37 |
| 9 | Isopropylbenzene | 0.28 | 0.0025 | 61 | | 0.16 |
| 9 | n-Propylbenzene | 0.37 | 0.0033 | 52 | | 0.17 |
| 10 | 1,2,3,5-Tetramethylbenzene | 3.98 | 0.0323 | 28 | | 0.90 |
| 11 | 1-Methylnaphthalene | 1.59 | 0.0122 | 25 | | 0.30 |
| Isoalkanes | | | | | | |
| 6 | 2-Methylpentane | 3.03 | 0.0382 | 14 | | 0.54 |
| 7 | 2-Methylhexane | 6.10 | 0.0662 | 4.4 | | 0.29 |
| 8 | 3-Methylheptane | 11.77 | 0.1120 | 1.5 | | 0.16 |
| 9 | 2-Methyloctane | 6.68 | 0.0567 | 0.48 | | 0.027 |
| Cycloparaffins | | | | | | |
| 6 | Cyclohexane | 10.30 | 0.1331 | 55 | | 7.32 |
| 7 | Methylcyclohexane | 10.00 | 0.1108 | 17 | | 1.88 |
| 8 | Dimethylcyclohexane | 2.25 | 0.0219 | 8.4 | | 0.184 |
| 9 | Isopropylcyclohexane | 4.28 | 0.0369 | 3.1 | | 0.114 |
| n-Alkanes | | | | | | |
| 5 | n-Pentane | 1.40 | 0.0211 | 38 | | 0.802 |
| 6 | n-Hexane | 2.95 | 0.0372 | 9.5 | | 0.354 |
| 7 | n-Heptane | 4.90 | 0.0531 | 3.4 | | 0.181 |
| 8 | n-Octane | 4.20 | 0.0400 | 0.41 | | 0.0164 |
| 9 | n-Nonane | 3.00 | 0.0255 | 0.22 | | 0.0056 |
| 10 | n-Decane | 2.88 | 0.0220 | 0.052 | | 0.0011 |
| 11 | n-Undecane | 3.09 | 0.0215 | 0.0044 | | 9.48E-05 |
| 12 | n-Dodecane | 2.67 | 0.0170 | 0.0037 | | 6.30E-05 |
| 13 | n-Tridecane | 2.03 | 0.0120 | 0.0029 | | 3.47E-05 |
| 14 | n-Tetradecane | 0.97 | 0.0053 | 0.0022 | | 1.17E-05 |
| TOTAL | | 100 | 1.0000 | | | 60.9 |

*Naphthalene has a fugacity ratio of 3.3 (solid at 25 C)

## 3. Endpoint for Modeling Remediation

The most stringent interpretation of the cleanup requirement for residual NAPL in the aquifers is to reduce the mole fraction of components of concern to fractions that yield equilibrium groundwater concentrations equal to or below RAOs or PRGs for groundwater. For benzene, the mole fraction yielding an MCL concentration of 5 µg/L at ambient temperature is 0.0000028 based on Raoult's Law:

$$y_{MCL,benzene} = \frac{C_{MCL}}{C^{sat}} = \frac{\left(0.005\frac{mg}{L}\right)}{\left(1790\frac{mg}{L}\right)} = 0.0000028$$

As indicated in Tables 4 and 5, the benzene fraction in untreated NAPL at ST012 is more than three orders of magnitude above this mole fraction. Remedial processes cannot selectively remove benzene; however, the reduction in mole fraction will be preferential for dissolution as benzene is the most soluble compound in the NAPL. For naphthalene, the mole fraction yielding the HBGL concentration of 28 µg/L at ambient temperature is 0.00027 based on Raoult's Law. The solubility of pure naphthalene is about 31 mg/L, but naphthalene is already dissolved as a liquid in the NAPL and the solubility in the water is enhanced according to its fugacity ratio (f) (Mukherji et al., 1997):

$$y_{HBGL,naphthalene} = \frac{C_{HBGL}}{C^{sat} f_N} = \frac{\left(0.028\frac{mg}{L}\right)}{\left(31\frac{mg}{L}\right)(3.3)} = 0.00027$$

The initial naphthalene mole fraction is just over one order-of-magnitude high but naphthalene has the potential to increase in mole fraction if more soluble compounds preferentially dissolve over time and the mass fraction of naphthalene increases in the NAPL as observed in the UWBZ. The equilibrium concentrations are calculated similarly for the other model NAPL components.

## 4. Idealized NAPL Depletion Assuming Groundwater-NAPL Equilibrium

As a first approximation for the time to attain RAOs, the depletion process can be idealized by assuming the NAPL consists of only two components: benzene dissolved in an otherwise insoluble NAPL. A further assumption of equilibrium between the NAPL and groundwater following Raoult's Law relates the groundwater concentration to the mass (mole) fraction of benzene in the depleting NAPL. A mass balance for the NAPL yields the benzene concentration over time as presented in Appendix A. This idealized expression for the time of remediation is,

$$t_{RAO} = \frac{-M_{Benzene} m_{NAPL,0}}{C^{sat}_{Benzene} \bar{M}_{NAPL}[Q + (1 - S_N)\varphi V_S \lambda_{Benzene}]} ln\left(\frac{C_{RAO}}{C_{Benzene,0}}\right)$$

The variables are defined in Appendix A. C represents the benzene concentration, M is molecular weight, m is the initial mass of the NAPL, Q is the flow through soil volume V, S is NAPL saturation, λ is a first order decay constant.

As an example, consider the soil volume targeted for EAB in the LSZ with the NAPL volume estimate from TPH concentrations and a porosity of 0.3 as presented in Table 3. Assume all components all insoluble except benzene,

$$m_{NAPL,0} = (54{,}821\ gal)\left(6.57\frac{lbs}{gal}\right)\left(0.4536\frac{kg}{lbs}\right) = 163{,}373\ kg$$

$$Q = \left(3.5\ \frac{gal}{min}\right)\left(0.0037854\frac{m^3}{gal}\right)\left(60 * 24\frac{min}{day}\right) = 19.08\frac{m^3}{day}$$

$$(1 - S_N)\varphi V_S = (1 - 0.0235)(0.3)(38{,}500\ cy)\left(0.76455\ \frac{m^3}{cy}\right) = 8{,}623\ m^3$$

$$M_{Benzene} = 78.114\ \frac{kg}{kmol}$$

$$\bar{M}_{NAPL} = 108.8\ \frac{kg}{kmol}$$

$$C_{Benzene}^{sat} = 1{,}790\ \frac{mg}{L}$$

$$S_N = 0.0235$$

$$\lambda_{Benzene} = 0.0125\ \frac{1}{day}$$

$$C_{RAO} = 0.005\ \frac{mg}{L}$$

$$C_{Benzene,0} = y_{Benzene,0}C_{Benzene}^{sat} = 20.7\ \frac{mg}{L}$$

$$t_{RAO} = \frac{-\left(78.114\ \frac{kg}{kmol}\right)(163{,}373\ kg)\left(10^{-6}\ \frac{mg}{kg}\right)\left(10^{-3}\ \frac{m^3}{L}\right)}{\left(108.8\ \frac{kg}{kmol}\right)\left(1{,}790\ \frac{mg}{L}\right)\left[19.08\frac{m^3}{day} + (8{,}623\ )(0.0125)\frac{m^3}{day}\right]} ln\left(\frac{0.005}{20.7}\right)$$

$$t_{RAO} = 4{,}302\ days = 11.8\ years$$

Hence, if the NAPL and groundwater maintain equilibrium and the degradation rate can be sustained at 0.0125 $d^{-1}$, MCL for benzene would be achieved in about 12 years. Idealized time of remediation results for the target EBR soil volumes and NAPL volumes in the UWBZ and LSZ are presented in Table 6. The input consisted of the volumes in Table 3, the ambient flows in Table 2, and the benzene solubility and initial mole fractions in Tables 4 and 5. The decay constants of 0.0125 $d^{-1}$ and 0.03 $d^{-1}$ are those suggested for EBR by sulfate reduction (Amec,

RD/RA Work Plan, 2014, Addendum 2, 2016). As indicated, the TOR ranged from 10 to 20 years in UWBZ and 8 to 27 years in the LSZ for a decay constant of 0.0125 $d^{-1}$. Calculations with a decay constant of 0.03 $d^{-1}$ yielded shorter timeframes as presented in Table 6. For comparison, the final two rows provide results for a decay constant of 0.00038 $d^{-1}$ (5 year half-life) expected to be representative of current methanogenic conditions (BEM, 2011) and display a rough order-of-magnitude increase in the TOR. These ranges provide ballpark numbers for assessing results when the assumptions are relaxed (e.g., multiple dissolving components in the NAPL, groundwater-NAPL dis-equilibrium, Monod kinetics for degradation).

**Table 6. Idealized NAPL Equilibrium Time of Remediation for Benzene**

| Aquifer Zone | Calculated Target NAPL Volume Porosity=0.3 years | Calculated Target NAPL Volume Porosity=0.4 years | Literature Target NAPL Volume Porosity=0.3 years | Literature Target NAPL Volume Porosity=0.4 years |
|---|---|---|---|---|
| **$\lambda_i$ = 0.0125 $d^{-1}$** | | | | |
| UWBZ | 16.1 | 10.4 | 19.0 | 19.5 |
| LSZ | 11.8 | 7.8 | 24.3 | 26.7 |
| **$\lambda_i$ = 0.03 $d^{-1}$** | | | | |
| UWBZ | 7.0 | 4.5 | 8.2 | 8.4 |
| LSZ | 5.4 | 3.5 | 11.1 | 12.0 |
| **$\lambda_i$ = 0.00038 $d^{-1}$** | | | | |
| UWBZ | 170 | 132 | 200 | 245 |
| LSZ | 67 | 55 | 136 | 182 |

## 5. Screening-Level NAPL Depletion Model

NAPL depletion can occur by natural attenuation processes. These processes include mass transfer from the NAPL, diffusion, dispersion in the groundwater flow field and natural degradation processes. After recovering mobile NAPL and partially depleting the residual NAPL through active remedial measures, three primary parameters are involved in the further depletion of components from the residual NAPL: flow rate, mass transfer from NAPL to water, and degradation rates (e.g., biological, oxidation, reduction). This section describes a NAPL depletion model that accounts for these processes using the same parameters as the NAPL Dissolution package provided in SEAM3D (Waddill and Widdowson, 2000). The mathematical derivation is described in Appendix B.

The depletion model treats the source zone as a single volume (or several blocks of varying treatment intensity interconnected by flow entering/exiting) rather than the multitude of discretized blocks found in a complex numerical model. A single volume block is illustrated in Figure 4. The depletion model results are equivalent in order of magnitude to more finely discretized numerical modeling results. Similar depletion models are described in peer-reviewed literature (Hansen & Kueper, 2007; Marble et al., 2008) and provide TOR estimates without implementing complex numerical models.

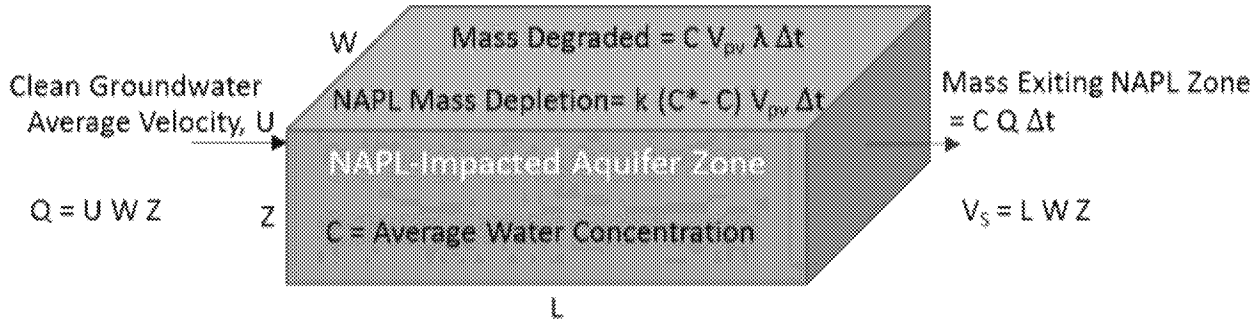


**Figure 4. Conceptual Model for Source Zone NAPL Depletion**

The governing equations for numerical modeling of a multi-component NAPL in saturated soil are (Waddill & Widdowson, 2000),

$$-\frac{\partial}{\partial x_j}(v_j C_i) + \frac{\partial}{\partial x_j}\left(D_{jk}\frac{\partial C_i}{\partial x_k}\right) + \frac{q}{\theta}C_i^* - r_i^{bio} + k_{N,i}(C_i^{eq} - C_i) = R_i\frac{\partial C_i}{\partial t}$$

$$\frac{\rho_b}{\phi}\frac{\partial C_i^N}{\partial t} = -k_{N,i}(C_i^{eq} - C_i)$$

The symbols are defined in Appendix B and the subscript i represents the ith component in the NAPL. From left to right, the terms in the first equation describe advection, dispersion, injection/extraction, biological degradation, mass transfer from residual NAPL, and partitioning by adsorption to soil solids. The second equation is a mass balance on the NAPL components transferred to the groundwater by dissolution. These equations can be averaged over the NAPL-impacted soil volume to define a single source term with NAPL that depletes with time according to the mass transfer rate coefficient $k_N$ and the concentration gradient. This single NAPL source represents an average for the input of multiple NAPL-impacted nodes in the full implementation of SEAM3D. Integrating the equations over the NAPL-impacted soil volume yields equations for the average dissolved concentration and the remaining NAPL mass or moles ($N_i$) for each NAPL component over time. Details of the derivation and underlying assumptions are presented in Appendix B and yield the following set of first order equations,

$$\frac{d\bar{C}_i}{dt} = -\frac{1}{R_i}\left[\frac{Q}{\phi V_S} + k_{N,i}\right]\bar{C}_i - \frac{\bar{r}_i^{bio}}{R_i} + \left[\frac{k_{N,i}C_i^{sat}}{R_i N_{total}^N}\right]N_i^N$$

$$\frac{dN_i^N}{dt} = -\left[\frac{\phi V_S k_{N,i}C_i^{sat}}{M_i N_{total}^N}\right]N_i^N + \left[\frac{\phi V_S k_{N,i}}{M_i}\right]\bar{C}_i$$

This representation is similar to Hansen & Kueper (2007) and Marble et al. (2008); however, the volume-averaged biological degradation is not found in those models. For a NAPL represented by 30 components, the number of equations to solve simultaneously is then 60 (dissolved phase concentration and number of moles in the NAPL for each component). The equations are interdependent as the equilibrium concentrations are dependent on the mole fractions in the

NAPL through Raoult's Law. These equations are readily solved with Runge-Kutta methods and yield the depletion of the NAPL over time with only a small number of specified parameters. The model is run until the mole fraction of each compound of interest in the NAPL yields an equilibrium concentration equal to the remedial goal. Given an initial NAPL mass and composition in a given soil volume, $V_S$, with specified physical properties and degradation rates, the equations demonstrate that NAPL depletion is governed by three parameters: (1) flow, Q, (2) the NAPL mass transfer rate coefficient $k_N$, and (3) degradation rates. For first order degradation, the rate is represented by a rate constant, $\lambda_i$,

$$\bar{r}_i^{bio} = (1 - S_N)\lambda_i \bar{C}_i$$

Alternative degradation kinetics are described in Appendix A for zero order and Monod kinetics when conditions are not accurately represented by a first order decay constant. Monod kinetics requires the addition of two first order equations to the system: a mass bass balance on the electron acceptor (E) and a mass balance on the microbial population ($M_{ec}$) as summarized below, with other variables defined in Appendix B,

$$\bar{r}_i^{bio} = \frac{M_{ec}}{\phi} G_i^e$$

$$\frac{d\bar{E}}{dt} = -\left[\frac{Q}{\phi V_S}\right]\bar{E} + \left[\frac{Q}{\phi V_S}\right] C_{bkgrnd}^{EA} - \frac{M_{ec}\gamma^e}{\phi}\sum_i G_i^e$$

$$\frac{dM_{ec}}{dt} = M_{ec}\left[-\lambda_{ec}^d + Y^e \sum_i G_i^e\right]$$

$$G_i^e = v_{i,e}^{max}\left(\frac{\bar{E}}{K_e + \bar{E}}\right)\left(\frac{\bar{C}_i}{K_i^e + \bar{C}_i}\right)$$

### *5.1. NAPL Depletion Calculations for First Order Degradation*

For the multi-component NAPL (31 components) described in Tables 3 and 4 for the UWBZ and LSZ, respectively, assuming first order degradation, and including mass transfer between the NAPL and groundwater, the equations to be solved are,

$$\frac{d\bar{C}_i}{dt} = -\frac{1}{R_i}\left[\frac{Q}{\phi V_S} + k_{N,i} + (1 - S_N)\lambda_i\right]\bar{C}_i + \left[\frac{k_{N,i}C_i^{sat}}{R_i N_{total}^N}\right] N_i^N$$

$$\frac{dN_i^N}{dt} = -\left[\frac{\phi V_S k_{N,i} C_i^{sat}}{M_i N_{total}^N}\right] N_i^N + \left[\frac{\phi V_S k_{N,i}}{M_i}\right]\bar{C}_i$$

Other than individual compound properties in Tables 4 and 5, the only additional system parameter required beyond equilibrium modeling, is the mass transfer coefficient, $k_N$. For screening, this property is assumed to be equal for all soluble components. Based on the work

of Mobile et al. (2016) where a range from 0.022 to 0.6 $d^{-1}$ was reported for forced flow conditions, a base value of 0.05 $d^{-1}$ is assumed for ambient conditions. Higher values push the solution toward the equilibrium assumption while lower values slow the process further.

Calculated times of remediation based on depleting benzene from NAPL to levels equivalent to MCL are presented in Table 7. NAPL models of the UWBZ and LSZ in Tables 4 and 5, respectively, were input along with the volumes and ambient flows in Tables 2 and 3. A first order decay constant of 0.0125 $d^{-1}$ was input for all calculations. The idealized times for groundwater equilibrium (=) are included from Table 6 for comparison. Results were not strongly sensitive to the mass transfer coefficient until the value was lowered to 0.005 $d^{-1}$. Times were faster than idealized equilibrium in some cases because the two-component model did not include the dissolution of other compounds that yielded in a higher benzene mole fraction over time in the multi-component model than in the 2-component model.

**Table 7. TOR for NAPL Depletion with First Order Degradation**
(Degradation Decay Constant = 0.0125 $day^{-1}$)

| Aquifer Zone | Mass Transfer Coefficient, $k_N$ 1/day | Calculated Target NAPL Volume Porosity=0.3 years | Calculated Target NAPL Volume Porosity=0.4 years | Literature Target NAPL Volume Porosity=0.3 years | Literature Target NAPL Volume Porosity=0.4 years |
|---|---|---|---|---|---|
| UWBZ - Equil | | 16.1 | 10.4 | 19.0 | 19.5 |
| UWBZ | 0.05 | 17.0 | 11.4 | 19.8 | 20.3 |
| UWBZ | 0.5 | 14.7 | 9.9 | 17.0 | 17.3 |
| UWBZ | 0.005 | 37.7 | 24.4 | 44.2 | 44.9 |
| LSZ - Equil | | 11.8 | 7.8 | 24.3 | 26.7 |
| LSZ | 0.05 | 13.7 | 9.4 | 26.9 | 29.2 |
| LSZ | 0.5 | 11.9 | 8.4 | 22.6 | 24.4 |
| LSZ | 0.005 | 31.7 | 20.8 | 64.2 | 68.6 |

### *5.2. NAPL Depletion Calculations for Sulfate Reduction with Monod Kinetics*

First order degradation is not expected to be applicable over the full range of hydrocarbon concentrations or the injection of sulfate into the subsurface for EBR. Therefore, the depletion model was also run including Monod kinetics for the multi-component NAPL (31 components) described in Tables 4 and 5 for the UWBZ and LSZ, respectively. Including mass transfer between the NAPL and groundwater and adding mass balances for sulfate ($C^e$) and biomass concentration ($M_{ec}$), the system of equations to be solved are,

$$\frac{d\bar{C}_i}{dt} = -\frac{1}{R_i}\left[\frac{Q}{\phi V_S} + k_{N,i}\right]\bar{C}_i - \frac{\bar{r}_i^{bio}}{R_i} + \left[\frac{k_{N,i}C_i^{sat}}{R_i N_{total}^N}\right]N_i^N$$

$$\frac{dN_i^N}{dt} = -\left[\frac{\phi V_S k_{N,i}C_i^{sat}}{M_i N_{total}^N}\right]N_i^N + \left[\frac{\phi V_S k_{N,i}}{M_i}\right]\bar{C}_i$$

$$\frac{d\bar{E}}{dt} = -\left[\frac{Q}{\phi V_S}\right]\bar{E} + \left[\frac{Q}{\phi V_S}\right] C_{bkgrnd}^{EA} - \frac{M_{ec}\gamma^e}{\phi}\sum_i G_i^e$$

$$\frac{dM_{ec}}{dt} = M_{ec}\left[-\lambda_{ec}^d + Y^e \sum_i G_i^e\right]$$

$$\bar{r}_i^{bio} = \frac{M_{ec}}{\phi} G_i^e$$

$$G_i^e = v_{i,e}^{max}\left(\frac{\bar{E}}{K_e + \bar{E}}\right)\left(\frac{\bar{C}_i}{K_i^e + \bar{C}_i}\right)$$

Additionally, the formulation assumes nutrients are not limiting and only sulfate reduction is applicable and the biomass yield coefficient, Y, is equal for all hydrocarbons. These equations also require two auxiliary relationships to constrain microbial population growth. The microbial population ($M_{ec}$) is assumed to grow when an excess of sulfate is available in comparison to the dissolved hydrocarbon mass. The microbial growth stops when insufficient hydrocarbon mass is available. Mathematically, this condition is represented by (Waddill & Widdowson, 2000),

$$If \left[ M_{SRB} \geq \sum_i Y_i^{SO_4^{2-}} \bar{C}_i \right] then \quad G_{SRB} = \sum_i G_i^e = 0$$

In general, the effective death rate is zero with an excess of sulfate and sufficient hydrocarbon mass. As the sulfate and/or hydrocarbon mass deplete to low levels, the microbial population begins to die off at a "background" rate. Mathematically, these conditions are represented by (Waddill & Widdowson, 2000),

$$\lambda_{SRB}^d = maximum\left[0, \lambda_{SRB}^{d,bk} - G_{SRB}\right]$$

Nomenclature:

$M_{SRB}$ = mass of microbial population (SRB) per bulk volume of aquifer
$\gamma^{SO_4^{2-}}$ = sulfate use coefficient for mass of sulfate per mass of hydrocarbon
$v_{i,SO_4^{2-}}^{max}$ = maximum specific rate of hydrocarbon i utilization for SRB population
$K_{SO_4^{2-}}$ = effective half − saturation constant for sulfate
$K_i^{SO_4^{2-}}$ = effective half − saturation constant for hydrocarbon i using sulfate
$\lambda_{SRB}^d$ = effective death rate of SRB microbial population
$\lambda_{SRB}^{d,bk}$ = background death rate of SRB microbial population
$Y_i^{SO_4^{2-}}$ = biomass yield coefficient (mass of microcolony per mass of substrate i)

The additional parameters required to model Monod kinetics are listed in Table 8. The sulfate use coefficient, maximum specific rate of hydrocarbon utilization, half-saturation constants, and biomass yield coefficient are referenced in BEM (Appendix M, 2011). The initial biomass concentration and background decay rate were employed in the BEM modeling (Appendix M, 2007). The biomass growth was limited to a critical value when dissolved hydrocarbon mass was insufficient to support further growth as described in the SEAM3D User Manual, "restrictions on microbial growth may be needed to simulate sites where engineered systems provide nutrients and EAs to an aquifer for enhanced bioremediation."

**Table 8. Parameters for Monod Kinetics**

| Parameter | | UWBZ | LSZ | Reference |
|---|---|---|---|---|
| $V_{Soil}$ | yd^3 | 122,556 | 38,500 | Table 2 |
| Q | gpm | 4.4 | 3.5 | Table 2 |
| $k_{NAPL}$ | 1/day | 0.05 | 0.05 | Mobile et al. (2016) |
| $C^{O2}$ (backgrnd) | mg/L | 7.0 | 7.0 | Table M.4.3.2.1 |
| $C^{NO3-}$ (backgrnd) | mg/L | 8.0 | 8.0 | Table M.4.3.2.1 |
| $C^{SO4-}$ (backgrnd) | mg/L | 200 | 290 | Table M.4.3.2.1 |
| $\gamma^{SO4-}$ | g/g | 4 | 4 | Table M.4.3.5.3 |
| $v^{max}_{Benzene,SO_4^{2-}}$ | 1/day | 0.000875 | 0.0175 | Table M.4.3.5.1/2 |
| $v^{max}_{Toluene,SO_4^{2-}}$ | 1/day | 0.001125 | 0.0225 | Table M.4.3.5.1/2 |
| $v^{max}_{Ethylbenzene,SO_4^{2-}}$ | 1/day | 0.000875 | 0.0175 | Table M.4.3.5.1/2 |
| $v^{max}_{Xylenes,SO_4^{2-}}$ | 1/day | 0.001125 | 0.0225 | Table M.4.3.5.1/2 |
| $v^{max}_{Naphthalene,SO_4^{2-}}$ | 1/day | 0.000125 | 0.0025 | Table M.4.3.5.1/2 |
| $v^{max}_{TMB,SO_4^{2-}}$ | 1/day | 0.000125 | 0.00125 | Table M.4.3.5.1/2 |
| $v^{max}_{Other\ Aromatics,SO_4^{2}}$ | 1/day | 0.000625 | 0.0125 | Table M.4.3.5.1/2 |
| $K_{SO_4^{2-}}$ | mg/L | 1 | 1 | Table M.4.3.5.3 |
| $K_i^{SO_4^{2-}}$ | mg/L | 5 | 5 | Table M.4.3.5.3 |
| $Y$ | g/g | 0.2 | 0.2 | BEM (2007) |
| $M_{SRB,0}$ (initial) | mg/L | 0.01 | 0.01 | BEM (2007) |
| $\lambda^{d,bk}_{SRB}$ | 1/day | 0.001 / 0.0 | 0.001 / 0.0 | BEM (2007) |

Enhanced sulfate reduction requires the injection of sulfate dissolved in water. Each pound of dissolved aromatic compound utilizes ~4 pounds of sulfate, theoretically. To dissolve and treat aromatic compounds in the NAPL at ST012, Mass Estimate Worksheet "TEA Estimate" describes the assumption of 30% treatment of the NAPL mass. Hence, the sulfate requirement is found from multiplying the NAPL mass by 0.3 and then again by 4. The calculated sulfate mass for each target zone NAPL estimate is provided in Table 9 along with a calculation for the fully distributed sulfate concentration in the pore water of the respective target soil volume. As indicated in Table 9, the initial distributed sulfate concentrations range from 16,400 mg/L to 54,400 mg/L. All of these values exceed recommended maximums (250 mg/L [Cunningham et al., 2001]; 2,000 mg/L [Sutherson et al., 2011]) and exceed higher values observed to inhibit sulfate reduction (4,000 mg/L [Al-Zuhair et al., 2008]). The modeling optimistically employed an initial distributed sulfate concentration of 8,000 mg/L.

**Table 9. Initial EBR-Targeted Sulfate Mass and Concentration**

| Aquifer Zone | | Calculated^ Target NAPL Volume Porosity=0.3 gal | Calculated^ Target NAPL Volume Porosity=0.4 gal | Literature* Target NAPL Volume Porosity=0.3 gal | Literature* Target NAPL Volume Porosity=0.4 gal |
|---|---|---|---|---|---|
| UWBZ V = 122,556 cy | NAPL (gal) | 250,999 | 215,142 | 294,399 | 395,887 |
| | Sulfate (kg) = | 1,032,067 | 884,629 | 1,210,521 | 1,627,823 |
| | Sulfate (mg/L) = | 36,715 | 23,603 | 43,064 | 43,432 |
| LSZ V = 38,500 cy | NAPL (gal) | 54,821 | 46,989 | 110,682 | 155,783 |
| | Sulfate (kg) = | 225,415 | 193,211 | 455,106 | 640,554 |
| | Sulfate (mg/L) = | 25,527 | 16,410 | 51,538 | 54,404 |

Calculated times of remediation based on depleting benzene from NAPL with sulfate reduction to levels equivalent to MCL are presented in Table 10 using Monod kinetics and an initial sulfate concentration of 8,000 mg/L. The previous results with a first order decay constant of 0.0125 $day^{-1}$ from Table 7 are included for comparison. Calculations were performed under two conditions for the Monod kinetics: (1) injection of slug mixed to an initial distributed concentration of 8,000 mg/L and then subjected to ambient flow, and (2) injection of slug mixed to an initial distributed concentration of 8,000 mg/L and then subjected to continuous recirculation such that ambient flow through the soil volume was zero and the sulfate was retained. For the assumed conditions, the Monod kinetic model indicated sulfate reduction was capable of depleting the benzene from the NAPL in times on the order of a decade and shorter than predicted by a first order decay constant of 0.0125 $d^{-1}$. Depletion continued with the background sulfate and the increased biomass. The durations for sulfate depletion from the target soil volume and the associated residual benzene groundwater concentrations are described in the notes.

**Table 10. TOR for NAPL Depletion with Sulfate Reduction and Monod Kinetics**

| Aquifer Zone – Kinetics | Ambient Flow gpm | Calculated Target NAPL Volume Porosity=0.3 years | Calculated Target NAPL Volume Porosity=0.4 years | Literature Target NAPL Volume Porosity=0.3 years | Literature Target NAPL Volume Porosity=0.4 years | Note |
|---|---|---|---|---|---|---|
| UWBZ – 1st Order | 4.4 | 17.0 | 11.4 | 19.8 | 20.3 | Note 1 |
| UWBZ – Monod | 4.4 | 100 | 92 | 111 | 136 | Note 2 |
| UWBZ – Monod | 0.0* | 125 | 115 | 139 | 172 | Note 3 |
| LSZ – 1st Order | 3.5 | 13.7 | 9.4 | 26.9 | 29.2 | Note 1 |
| LSZ – Monod | 3.5 | 9.5 | 8.0 | 17.7 | 22.6 | Note 4 |
| LSZ – Monod | 0.0* | 10.6 | 8.6 | 18.2 | 22.7 | Note 5 |

* Zero ambient flow is included to mimic recirculation wherein sulfate is not lost with groundwater exiting the target soil volume.

Note 1: Calculated with a first order degradation rate constant of 0.0125 $d^{-1}$, assumed to be applicable for all time independent of sulfate concentration and biomass conditions.

Note 2: For a background death rate of 0.001 $d^{-1}$, the microbial population did not grow, the injected sulfate was not utilized, and the TOR was over 200 years based primarily on the dissolved phase exiting the source soil volume. Setting the background microbial death rate to 0 yielded a TOR of 92-136 years by allowing the biomass to grow slowly (limited by the utilization rate); very little of the injected sulfate was utilized.

Note 3: For a background death rate of 0.001 $d^{-1}$ and no ambient flow through the soil volume, the microbial population did not grow, injected sulfate was not utilized, and no degradation occurred (TOR is infinity). Setting the background death rate to 0 allowed the biomass to grow yielding a TOR of 115-172 years (limited by the low utilization rate).

Note 4: The initial distribution of excess sulfate (8,000 mg/L) was utilized or washed out of the soil volume in 3 to 3.6 years; however, the microbial concentration grew and utilized ambient sulfate entering the volume to complete the process along with dissolved mass flow out of the volume. Assuming a microbial background death rate of zero shortened the TOR by 1 to 2 years.

Note 5: The initial distribution of sulfate (8,000 mg/L) was sufficient to deplete benzene from the calculated residual NAPL; literature-based NAPL required 10,000 mg/L. Assuming a zero microbial background death rate shortened the TOR by 2 to 5 years.

Based on the model and underlying assumptions, the concentration of sulfate reducing bacteria grew to a stationary phase concentration around 3 to 3.5 mg/L in both zones, when growth occurred. The growth period was approximately 12 to 24 months in the LSZ. The growth period in the UWBZ was on the order of 35 to 40 years assuming a zero death rate. The UWBZ growth was slow and the results were very sensitive to the death rate as a result of the low utilization rate. The calculated TOR was not strongly influenced by the assumed initial biomass concentration (0.01 mg/L). Based on the model NAPL compositions, initial sulfate concentrations exceeding 8,000 mg/L provided no improvement in the TOR and concentrations above 4,000 mg/L may begin to inhibit sulfate reduction (Al-Zuhair et al., 2008).

Conditions in the UWBZ are known to be evolving (BEM, 2011); therefore, calculations for the UWBZ were repeated assuming subsurface conditions could be manipulated to improve utilization rates of hydrocarbons by a factor of ten over the calibrated values from 2011. The results are provided below in Table ES2.

**Table 11. TOR for UWBZ NAPL Depletion with Sulfate Reduction (Utilization x 10)**

| **Aquifer Zone – Kinetics** | **Ambient Flow** gpm | **Calculated Target NAPL Volume** Porosity=0.3 **years** | **Calculated Target NAPL Volume** Porosity=0.4 **years** | **Literature Target NAPL Volume** Porosity=0.3 **years** | **Literature Target NAPL Volume** Porosity=0.4 **years** |
|---|---|---|---|---|---|
| UWBZ – Monod ($\upsilon_i^{max}$ Table 8) | 4.4 | 100 | 92 | 111 | 136 |
| UWBZ – Monod ($\upsilon_i^{max}$x10) | 4.4 | 28.7 | 17.0 | 35.1 | 43.1 |

## 6. Phase I Feasibility and Implementation Issues

Based on the model and its output, study topics for the first phase of sulfate reduction at the site include:

1. Will engineered degradation rates yield attainment of remedial objectives in desired timeframes?
2. Will the sulfate reducing bacteria (SRB) biomass grow as needed?
3. What is the optimal concentration for sulfate injection?
4. Will highly concentrated injections of sulfate be inhibitive to bacterial activity?
5. Will the injected sulfate become well distributed with respect to NAPL accumulations?
6. What is the lag time for SRB to acclimate to elevated sulfate concentrations (not included in the model)?
7. Inhibition by other degradation processes and nutrient availability are not included in the model, are these factors important?
8. Will hydrogen sulfide concentrations or other reaction products inhibit degradation or will subsurface conditions mitigate their buildup?
9. If/when sulfate is no longer limiting rates of degradation, what will limit the reaction and what degradation rates can be expected?
10. Is benzene slower to degrade than other aromatics, or faster, or average?
11. Will periodic sulfate injections or recirculation be necessary to sustain degradation rates?
12. How will the actual depletion of aromatic compounds from NAPL be assessed>

## References


Al-Zuhair, S., M.H. El-Naas, and H. Al-Hassani, 2008, "Sulfate inhibition effect on sulfate reducing bacteria," Journal of Biochemical Technology, 1(2) pp 39-44.

Aronson, D. and P.H. Howard, 1997, "Anaerobic Biodegradation of Organic Chemicals in Groundwater: A Summary of Field and Laboratory Studies, Final Report" prepared for American Petroleum Institute by Syracuse Research Center. Available at http://www.energytomorrow.org/~/media/files/ehs/clean_water/gw_other/anerobicbiodegrateconstantrpt1998.pdf

Basu, N.B., A.D. Fure, and J.W. Jawitz, 2008, "Predicting dense nonaqueous phase liquid dissolution using a simplified source depletion model parameterized with partitioning tracers," Water Resources Research, 44(7): W07414.

Bekins, B.A., Warren, E., and Godsy, E.M., 1998, "A comparison of zero-order, first-order, and monod biotransformation models," Ground Water, v. 36(2) pp. 261 – 268.

BEM, 2007, Final Phase I Thermal Enhanced Extraction (TEE) Pilot Test Work Plan, November.

BEM, 2011, Final Phase I Thermal Enhanced Extraction (TEE) Pilot Test Performance Evaluation Report, March.

Brauner, J.S., and M.A. Widdowson. 2001. Numerical simulation of a natural attenuation experiment with a petroleum hydrocarbon NAPL source. Ground Water 39, no. 6: 939–952.

Chappelle, F.H. 2001. Ground-Water Microbiology and Geochemistry, 2nd ed. New York: John Wiley & Sons Inc.

Chappelle, F.H., Bradley, P.M., Lovely, D.R., O'Neill, K. and Landmeyer, J.E., 2002. Rapid evolution of redox processes in a petroleum hydrocarbon-contaminated aquifer. Ground Water, 40(4), 353-360.

Chappelle, F.H., M.A. Widdowson, J.S. Brauner, E. Mendez and C.C. Casey, 2003, Methodology for Estimating Times of Remediation Associated with Monitored Natural Attenuation. USGS Water Resources Investigation Report 03-4057. Available at http://pubs.usgs.gov/wri/wri034057/pdf/wrir03-4057.pdf

Clement, T., T. Gautam, K.K. Lee, M. Truex, and G. Davis, 2004, "Modeling of DNAPL-Dissolution, Rate-Limited Sorption and Biodegradation Reactions in Groundwater Systems," Bioremediation Journal, 8(1–2): 47–64.

Cunningham, J., H. Rahme, G. Hopkins, C. Lebron, and M. Reinhard, 2001, "Enhanced In Situ Bioremediation of BTEX-Contaminated Groundwater by Combined Injection of Nitrate and Sulfate," Environmental Science & Technology, 35(8): 1663–1670.

Eweis, J.B., S.J. Ergas, D. P. Y. Chang, and E.D. Schroeder. 1998. Bioremediation Principles. McGraw-Hill, Boston, MA.

Hansen, S. and B. Kueper, 2007, "An analytical solution to multi-component NAPL dissolution equations," Advances in Water Resources, Vol 30, Issue 3, pp 382-388.

ITRC, 2009. Evaluating Natural Source Zone Depletion at Sites with LNAPL, Interstate Technology and Regulatory Council, Washington, D.C.

Johnson, P., P. Lundegard and Z. Liu, 2006, "Source Zone Natural Attenuation at Petroleum Hydrocarbon Spill Sites – I: Site-Specific Assessment Approach," Ground Water Monitoring & Remediation, 26(4), 82-92.

Marble, J.C., E. L. DiFilippo, Z. Zhang, G. R. Tick, and M. L. Brusseau, 2008, "Application of a Lumped-Process Mathematical Model to Dissolution of Non-Uniformly Distributed Immiscible Liquid in Heterogeneous Porous Media," J Contam Hydrol. 2008 August 20; 100(1-2): 1–10.

Mayer, A.S., and C.T. Miller, 1996, "The influence of mass transfer characteristics and porous media heterogeneity on nonaqueous phase dissolution," Water Resources Research, 32(6), 1551-1567.



ED_005025_00013390-00021

Miller, C.T., Poirier-McNeill, M.M., Mayer, A.S., 1990. Dissolution of trapped nonaqueous phase liquids: Mass transfer characteristics. Water Resources Research, 26(11), 2783-2796.

Mobile, M., M. Widdowson, and D. Gallagher, 2012, "Multicomponent NAPL Source Dissolution: Evaluation of Mass-Transfer Coefficients," Environ. Sci. Technol., 46 (18), pp 10047–10054.

Mobile, M, M Widdowson, L Stewart, J Nyman, R Deeb, M Kavanaugh and D Gallagher, 2016, "In-Situ Determination of Field-Scale NAPL Mass Transfer Coefficients: Performance, Simulation and Analysis," accepted for publication in Journal of Contaminant Hydrology.

Mukherji, S., C. Peters, and W. Weber, 1997, "Mass Transfer of Polynuclear Aromatic Hydrocarbons from Complex DNAPL Mixtures," Environmental Science & Technology, 31(2), pp 416-423.

Sutherson, S., K Houston, M Schnobrich and J. Horst, 2011, "Engineered Anaerobic Bio-Oxidation Systems for Petroleum Hydrocarbon Residual Source Zones with Soluble Sulfate Application," Ground Water Monitoring & Remediation, 31(3), pp 41-46.

U.S. Environmental Protection Agency (USEPA), 1999, "Anaerobic Biodegradation Rates of Organic Chemicals in Groundwater: A Summary of Field and Laboratory Studies,"

Waddill, D. and M. Widdowson, 2000, "SEAM3D: A Numerical Model for Three-Dimensional Solute Transport and Sequential Electron Acceptor-Based Bioremediation in Groundwater," ERDC/EL TR-00-18, November 2000.



ED_005025_00013390-00022

## Appendix A
# Depletion of Two-Component NAPL Assuming Equilibrium

If the mass transfer coefficient between NAPL and groundwater is very high, we can assume the groundwater is in equilibrium with the NAPL leaving only a mass balance on the NAPL for a solution. The groundwater concentration is equal to the equilibrium concentration through Raoult's Law,

$$C_1 = \frac{N_1^N}{N_{total}^N} C_i^{sat} = y_1 C_1^{sat}$$

Assume the NAPL consists only of a water soluble component 1 at low mass fraction with the remaining mass made up of insoluble component 2. The total mass of a two-component NAPL can be expressed as,

$$m_{NAPL} = m_1 + m_2 = N_1 M_1 + N_2 M_2$$

$$N_{NAPL} = N_1 + N_2$$

$$m_{NAPL} = m_1 + m_2 = N_{NAPL}(y_1 M_1 + y_2 M_2)$$

m is mass, M is molecular weight, N are moles and y are mole fractions. Component 2 is insoluble so that the mass does not change and assume this mass is significantly larger than the mass of component 1 in the NAPL. Then, we find approximately,

$$\Delta m_{NAPL} = \Delta m_1 = \Delta y_1 M_1 N_{NAPL,0}$$

Conservation of mass in the averaged volume yields,

$$Change\ in\ NAPL\ mass = -Mass\ Extracted - Mass\ Degraded$$

$$\Delta m_{NAPL} = -Q C_1 \Delta t - (1 - S_N)\varphi V_S \lambda_1^e C_1 \Delta t$$

$$M_1 N_{NAPL,0} \frac{\Delta y_1}{\Delta t} = -[Q + (1 - S_N)\varphi V_S \lambda_1^e] C_1$$

$$\frac{dy_1}{dt} \cong -\left[\frac{Q + (1 - S_N)\varphi V_S \lambda_1^e}{M_1 N_{NAPL,0}}\right] C_1^{sat} y_1$$

$$y_1 = y_{1,0} exp\left\{\left[\frac{-Q - (1 - S_N)\varphi V_S \lambda_1^e}{M_1 N_{NAPL,0}}\right] C_1^{sat} t\right\}$$

$$C_1 = y_{1,0} C_1^{sat} exp\left\{-[Q + (1 - S_N)\varphi V_S \lambda_1^e]\left(\frac{\overline{M}_{NAPL} C_1^{sat}}{M_1 m_{NAPL,0}}\right) t\right\}$$

The calculation for time to a specific average groundwater concentration is then,

$$t_{RAO} = \frac{-M_1 m_{NAPL,0}}{C_1^{sat}\bar{M}_{NAPL}[Q + (1 - S_N)\varphi V_S \lambda_1^e]} ln\left(\frac{C_{RAO}}{C_{1,0}}\right)$$

## Appendix B
## Volume-Averaged Depletion of Multi-Component NAPL Source Zones

Most sites lack the characterization details of NAPL architecture that would make numerical modeling meaningful in predicting the fate of NAPL sources zones. Recent advances in specifying a NAPL source are available with SEAM3D (Waddill & Widdowson, 2000) but require specification of the full transport and degradation domain and a numerical solution. At the feasibility study level, a method to compare order-of-magnitude effectiveness and the long-term impact of disparate technologies and approaches that does not require a major modeling effort is desirable. Numerous screening level models exist to calculate the downgradient dissolved plume (e.g., BIOSCREEN) and estimate source life with uncorrelated parameters (e.g., REMFuel); however, off-the-shelf screening model are not readily available to estimate the time of benzene depletion from a multi-component NAPL using field variables. Starting with an initial NAPL mass in a specified source volume and applying remedial alternative-specific parameters for NAPL dissolution, extraction, and in situ degradation/destruction yields screening level estimates of NAPL depletion over time with a minimal number of inputs. These order-of-magnitude estimates follow the approaches described by Johnson et al. (2006) and Chappelle et al. (2003) for monitored natural attenuation in NAPL source zones.

### Governing Equations

Consider the three-dimensional, transient transport of contaminants dissolving from an immobile, multi-component NAPL dispersed in an aquifer. The governing equations including aqueous phase biological (or other) reactions are (Waddill & Widdowson, 2000; Clement et al., 2004),

$$\frac{\partial C_i}{\partial t} + \frac{\rho_b}{\phi}\frac{\partial C_i^{ads}}{\partial t} = \frac{\partial}{\partial x_j}\left(D_{jk}\frac{\partial C_i}{\partial x_k}\right) - \frac{\partial}{\partial x_j}(v_j C_i) - r_i^{bio} - \frac{\rho_b}{\phi}\frac{\partial C_i^N}{\partial t}$$

$$\frac{\rho_b}{\phi}\frac{\partial C_i^{ads}}{\partial t} = \xi_i\left(C_i - \frac{C_i^{ads}}{k_{d,i}}\right)$$

$$\frac{\rho_b}{\phi}\frac{\partial C_i^N}{\partial t} = -k_{N,i}(C_i^* - C_i)$$

These equations represent the dissolution of component i from the NAPL ($C_i^N$ = concentration in the NAPL) into adjacent groundwater, its partitioning between the soil solids and groundwater

($C_i^{ads}$ = concentration adsorbed to solids), and its movement with groundwater through the aquifer ($C_i$ = dissolved concentration in water). Assuming instantaneous equilibrium between the dissolved and adsorbed concentrations (based on typical NAPL source zone dimensions and groundwater velocities) introduces the usual retardation coefficient (modified to include the NAPL saturation) and reduces the transport problem to two equations for the water and NAPL concentrations:

$$R_i \frac{\partial C_i}{\partial t} = \frac{\partial}{\partial x_j}\left(D_{jk}\frac{\partial C_i}{\partial x_k}\right) - \frac{\partial}{\partial x_j}(v_j C_i) - r_i^{bio} - \frac{\rho_b}{\phi}\frac{\partial C_i^N}{\partial t}$$

$$\frac{\rho_b}{\phi}\frac{\partial C_i^N}{\partial t} = -k_{N,i}(C_i^* - C_i)$$

$$R_i = 1 - S_N + \frac{\rho_b k_{d,i}}{\phi}$$

Additional nomenclature includes,

| | | |
|---|---|---|
| $v$ | = | seepage velocity of ground water |
| $S_N$ | = | NAPL saturation |

Biological degradation processes for terminal electron acceptors (TEA) are included in a simplified form assuming zero and first order degradation and/or Monod kinetics depending upon site conditions:

$$r_i^{bio} = \sum_{l}^{TEA} 0\ order + \sum_{m}^{TEA} 1st\ order + \sum_{n}^{TEA} Monod$$

Different processes may occur in different portions of the soil volume. The equation for the NAPL concentration represents a mass balance on the NAPL and therefore it is interdependent on the NAPL saturation $S_N$. In addition, the mass transfer coefficient $k_{N,i}$ is also dependent on the NAPL saturation (Miller et al., 1990) as well as the water velocity. $C^*_i$ represents the equilibrium concentration of component i in water governed by its pure component solubility and Raoult's law and thereby its concentration in the NAPL. Other assumptions include:

- NAPL is immobile
- concentration gradients within the NAPL mass itself resulting from surficial dissolution are ignored
- NAPL is non-wetting to the soil (the entire solid surface is available for adsorption)
- Biological degradation occurs solely in the dissolved phase

However, the assumptions for uniform NAPL distribution and homogeneous soils are not strictly applicable. In the derivation below, the mass transfer coefficient for the NAPL is defined to capture variability in distribution and heterogeneous flow by averaging over the source zone volume.



ED_005025_00013390-00025

To avoid complex numerical solutions, we can integrate over the NAPL contaminated soil volume to obtain a volume-averaged dissolved phase concentration within the source zone (Marble et al., 2008; Johnson et al., 2006). For illustration the NAPL-impacted soil volume is assumed to be rectangular ($V_s$ = HxWxL) and the groundwater flow unidirectional, however the volume can be of arbitrary shape defined by field conditions and the flow can be fully three-dimensional without limitation on the averaging. After integrating in the y- and z-directions and applying associated boundary conditions, the x-direction integration yields the following expressions,

$$R_i \frac{\partial \bar{C}_i}{\partial t} = \frac{1}{L}\int_{x'=0}^{L} \frac{\partial}{\partial x'}\left(D_{xx}\frac{\partial C_i}{\partial x'}\right) dx' - \frac{1}{L}\int_{x'=0}^{L} \frac{\partial}{\partial x}(v_x C_i) dx' - \bar{r}_i^{bio} - \frac{\rho_b}{\phi}\frac{d\bar{C}_i^N}{dt}$$

$$\frac{\rho_b}{\phi}\frac{d\bar{C}_i^N}{dt} = -k_{N,i}(C_i^* - \bar{C}_i)$$

The average dissolved phase concentration within the source zone soil volume is defined by,

$$\bar{C}_i = \frac{1}{HWL}\iiint C_i(x',y',z')dx'dy'dz' = \frac{1}{V_S}\iiint C_i(x',y',z')dx'dy'dz'$$

The averaging assumes biodegradation is uniform throughout the integrated volume. Assuming properties are uniform over the source zone volume, $V_s$, assuming the NAPL saturation varies slowly with time, and carrying out the integration in the dissolved phase governing equation yields,

$$R_i \frac{d\bar{C}_i}{dt} = \frac{D_{xx}}{L}\int_{x'=0}^{L} \frac{\partial}{\partial x'}\left(\frac{\partial C_i}{\partial x'}\right) dx' - \frac{v_x}{L}\int_{x'=0}^{L} \frac{\partial}{\partial x}(C_i) dx' - \bar{r}_i^{bio} + k_{N,i}(C_i^* - \bar{C}_i)$$

$$R_i \frac{d\bar{C}_i}{dt} = \frac{D_{xx}}{L}\frac{\partial C_i}{\partial x'}\bigg|_{x'=0}^{L} - \frac{v_x}{L}(C_i)|_{x'=0}^{L} - \bar{r}_i^{bio} + k_{N,i}(C_i^* - \bar{C}_i)$$

Assume the source zone is well mixed (i.e., concentration gradients are near zero and the exiting dissolved phase concentration equals the average concentration) and that water entering the source zone has a zero concentration to find,

$$R_i \frac{d\bar{C}_i}{dt} = -\frac{1}{L}(v_x \bar{C}_i) - \bar{r}_i^{bio} + k_{N,i}(C_i^* - \bar{C}_i)$$

$$R_i \frac{d\bar{C}_i}{dt} = -\left[\frac{Q}{\phi V_S}\right]\bar{C}_i - \bar{r}_i^{bio} + k_{N,i}(C_i^* - \bar{C}_i)$$

$$Q = v_x \phi W Z$$

Consider the definition of the NAPL phase concentration and rewrite the equation in terms of moles in place of mass,

$$\frac{\rho_b}{\phi}\frac{d\bar{C}_i^N}{dt} = \frac{\rho_b}{\phi}\frac{d}{dt}\left(\frac{m_i^N}{\rho_b V_S}\right) = \frac{1}{\phi V_S}\frac{dm_i^N}{dt} = \frac{M_i}{\phi V_S}\frac{dN_i^N}{dt}$$

Raoult's Law applied to the NAPL and water partitioning is written as,

$$C_i^* = \frac{N_i^N}{N_{total}^N} C_i^{sat}$$

Substituting yields two governing equations for two unknowns (dissolved phase concentration and number of moles in the NAPL) for each component of the NAPL,

$$\frac{d\bar{C}_i}{dt} = -\frac{1}{R_i}\left[\frac{Q}{\phi V_S} + k_{N,i}\right]\bar{C}_i + \left[\frac{k_{N,i}C_i^{sat}}{R_i N_{total}^N}\right]N_i^N - \frac{\bar{r}_i^{bio}}{R_i}$$

$$\frac{dN_i^N}{dt} = -\left[\frac{\phi V_S k_{N,i} C_i^{sat}}{M_i N_{total}^N}\right]N_i^N + \left[\frac{\phi V_S k_{N,i}}{M_i}\right]\bar{C}_i$$

To complete the problem specification, the mass (mole) balance for the multi-component NAPL defines the total number of moles in the NAPL and the average NAPL saturation,

$$N_{total}^N = \sum_i N_i^N = \sum_i \frac{m_i^N}{M_i}$$

$$S_N = \frac{m_{total}^N}{\rho_N \phi V_S} = \frac{1}{\rho_N \phi V_S}\sum_i m_i^N = \frac{1}{\rho_N \phi V_S}\sum_i M_i N_i^N$$

The coefficients are explicitly dependent on the NAPL saturation (i.e., total number of moles) along with the retardation and mass transfer coefficients. However, these parameters change slowly with time and can be held constant over small time steps with little loss in accuracy. The two governing equations are easily solved numerically using standard Runge-Kutta methods by holding the coefficients constant during a time step and then recalculating the coefficients using the new concentrations and mole fractions. Higher order schemes can increase accuracy. At the end of a time step, we can calculate the number of moles remaining and the new NAPL saturation along with an updated mass transfer coefficient (Clement et al., 2004),

$$k_{N,i} = k_{N,i}^0 \left(\frac{S_N}{S_N^0}\right)^\beta$$

If the NAPL has components that exist as a solid in pure phase at the system temperature (e.g., naphthalene), the equilibrium concentration includes a fugacity ratio and the new concentration must be checked to ensure it does not exceed the solubility limit of the solid phase before taking the next time step. If so, the concentration must be corrected to the solubility limit to avoid incorrect conditions suggesting precipitation.

## Biological Degradation Processes

In the volume-averaging above, the biological degradation processes are assumed to apply throughout the NAPL-impacted soil volume. Models of degradation include three types: zero order, first order and Monod kinetics. An example of a zero order process in the volume-averaged model is the entry of background electron acceptors into the soil volume where it is assumed they are instantaneously utilized. First order processes are commonly applied and assume the degradation is exponential proportional to a single decay rate constant and the dissolved hydrocarbon concentration. Monod kinetics include dependencies on electron acceptors, hydrocarbon concentrations, as well as biomass growth, nutrient availability, and inhibitions. Each degradation model is described below.

### *Zero Order Model*

Biological degradation processes limited by the availability of terminal electron acceptors (TEA) from upgradient sources include aerobic degradation (dissolved oxygen), nitrate reduction, and sulfate reduction. If TEA are completely depleted before exiting the source zone (independent of degradation location), the processes can be modeled as zero order in the volume-averaged approach. The TEA mass rate into the soil volume is the total groundwater flow entering multiplied by the upgradient TEA concentration. The mass rate of TEA is divided by stoichiometric use factors to estimate the total mass degradation rate of dissolved hydrocarbons,

$$\bar{r}_i^{zero} = \frac{Q}{\phi V_S}\left(\frac{\bar{E}_{O_2}^{bkgrnd}}{\gamma^{O_2}} + \frac{\bar{E}_{NO_3^-}^{bkgrnd}}{\gamma^{NO_3^-}} + \frac{\bar{E}_{SO_4^{2-}}^{bkgrnd}}{\gamma^{SO_4^{2-}}}\right) f_i$$

$$1 = \sum f_i \approx \sum \frac{\bar{C}_i}{\bar{C}_{Total}}$$

$$\bar{C}_{Total} = \sum \bar{C}_i$$

Nomenclature includes,

$\bar{E}_{TEA}^{bkgrnd}$ = upgradient concentration of TEA entering source zone (mg/L)
$\gamma^{TEA}$ = terminal electron acceptor use coefficient (g/g)

In this formulation, dissolved hydrocarbons are assumed to utilize the TEA in proportion to their concentrations. More detailed weighting strategies for utilization of TEA among the dissolved hydrocarbons could be employed. The electron acceptor use coefficients are based on average stoichiometric values for hydrocarbon oxidation (USEPA, 1998) and independent of individual compound.

$\gamma^{O2} = 3.1$ $\gamma^{NO3} = 3.0$ $\gamma^{SO4} = 4.0$

### *First Order Model*



ED_005025_00013390-00028

In first order processes, the degradation is assumed exponential according to a single decay rate constant and is proportional to the dissolved hydrocarbon concentration,

$$\bar{r}_i^{first} = (1 - S_N)\lambda_i^{TEA}\bar{C}_i$$

$\lambda_i^{TEA}$ = first-order degradation rate constant for the TEA process considered (1/day)

The NAPL occupies pore space (saturation) and is subtracted from the pore volume in which degradation occurs. This model is most often applied when the TEA are not limiting and the dissolved hydrocarbon concentration is low. Natural processes that most nearly occur throughout the source soil volume, assuming sufficient biomasses exist, include manganese reduction, iron reduction and methanogenesis. The manganese and iron reductions are reaction-rate limited and continue until the soil solids are depleted of these soluble electron acceptors. Methanogenesis is generally self-sustaining as it produces more carbon dioxide (the electron acceptor) than it consumes and therefore is limited by the rate of reaction and concentration of biomass but continues indefinitely.

***Monod Kinetics***

Monod kinetics should be used to model transient systems wherein degradation rates are expected to vary with changes in concentrations of hydrocarbons and/or electron acceptors. Assume a slug of TEA is injected and mixed to an average, uniform concentration instantaneously. Following the formulation in SEAM3D (Waddill & Widdowson, 2000), assuming nutrient availability, and ignoring inhibition, we write:

$$\bar{r}_i^{Monod} = \frac{M_{TEA}}{\phi} v_{i,TEA}^{max} \left(\frac{\bar{E}_{TEA}}{K_{TEA}^i + \bar{E}_{TEA}}\right)\left(\frac{\bar{C}_i}{K_i^{TEA} + \bar{C}_i}\right) = \frac{M_{TEA}}{\phi} G_i^{TEA}$$

$$G_i^{TEA} = v_{i,TEA}^{max} \left(\frac{\bar{E}_{TEA}}{K_{TEA}^i + \bar{E}_{TEA}}\right)\left(\frac{\bar{C}_i}{K_i^{TEA} + \bar{C}_i}\right)$$

$E_{TEA}$ is the dissolved concentration of TEA, $M_{TEA}$ represents the microbial concentration associated with the specific TEA, and other variables are,

$v_{i,TEA}^{max}$ = maximum specific rate of hydrocarbon i utilization for the microbial population
$K_{TEA}^i$ = effective half-saturation constant for TEA
$K_i^{TEA}$ = effective half-saturation constant for hydrocarbon i using TEA

A conservation equation is also required for the TEA concentration and volume-averaging yields,

$$\frac{d\bar{E}_{TEA}}{dt} = -\left[\frac{Q}{\phi V_S(1 - S_N)}\right]\left(\bar{E}_{TEA} - \bar{E}_{TEA}^{bkgrnd}\right) - \frac{M_{TEA}}{\phi}\sum_i \gamma_i^{TEA} G_i^{TEA}$$

$$\bar{E}_{TEA}(t = 0) = \bar{E}_{TEA}^0$$

The remaining unknown in the model is the microbial concentration. The microbial population ($M_{TEA}$) associated with the TEA is assumed to grow when an excess of TEA is available in comparison to the dissolved hydrocarbon mass. The growth of the microbial population, following the instantaneous introduction of excess TEA, is illustrated in the Figure below.

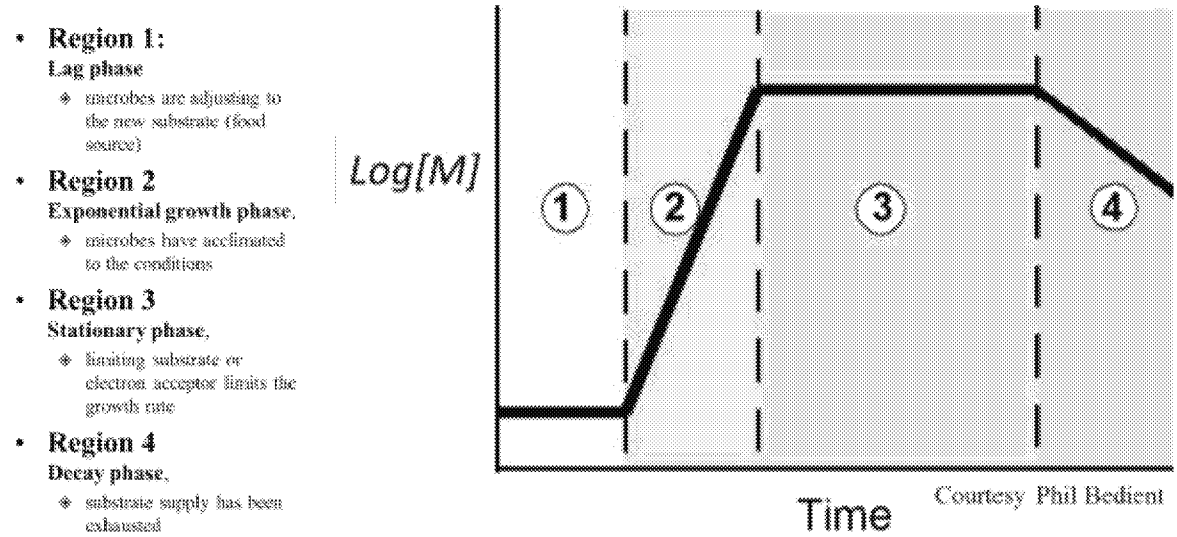


Illustration of Microbial Growth

Conservation of mass for the microbial growth and associated "effective" death, neglecting the lag phase shown in the figure above, yields

$$\frac{dM_{TEA}}{dt} = M_{TEA}\left[-\lambda_{TEA}^{d} + \sum_{i} Y_i^{TEA} G_i^{TEA}\right]$$

$$M_{TEA}(t=0) = M_{TEA}^{0}$$

$\lambda_{TEA}^{d}$ = effective death rate of microbial population associated with TEA
$Y_i^{TEA}$ = biomass yield coefficient (mass of microcolony per mass of utilized substrate i)

The microbial growth stops when insufficient hydrocarbon mass is available and the process enters the stationary phase. This condition is represented by (Waddill & Widdowson, 2000),

If $\left[\ M_{TEA} \geq \sum_i\ Y_i^{TEA}\bar{C}_i\ \right]$ then $Y_i^{TEA}G_i^{TEA}$ =0

In general, the effective death rate is zero with an excess of TEA and sufficient hydrocarbon mass. As the TEA and/or hydrocarbon mass deplete to low levels, the microbial population begins to die off at a "background" rate. This condition is represented by (Waddill & Widdowson, 2000),

$$\lambda_{TEA}^{d} = maximum\left[0, \lambda_{TEA}^{d,bkgrnd} - Y_i^{TEA}G_i^{TEA}\right]$$

For screening calculations we can assume the TEA use coefficient and the biomass yield coefficient are averages for the dissolved hydrocarbons.